



(RESEARCH ARTICLE)



Synthesis and *ab initio* Determination of $\text{Bi}_{1.25}\text{V}_{0.123}\text{Ca}_{0.245}\text{N}_{1.24}\text{O}_8$ cubic structure via powder X-ray diffraction data

Rohit kumar Dev and Parashuram Mishra *

Bioinorganic and Materials Chemistry Research Lab. M. M. A. M. Campus, Tribhuvan University Biratnagar, Nepal.

Publication history: Received on 01 September 2020; revised on 13 September 2020; accepted on 16 September 2020

Article DOI: <https://doi.org/10.30574/wjarr.2020.7.3.0333>

Abstract

This paper deals with the *ab initio* structure determination of $\text{Bi}_{1.25}\text{V}_{0.123}\text{Ca}_{0.245}\text{N}_{1.24}\text{O}_8$ cubic structure from powder X-ray data using the Rietveld method, and with physical properties characterization of a related solid solution. $\text{Bi}_{1.25}\text{V}_{0.123}\text{Ca}_{0.245}\text{N}_{1.24}\text{O}_8$ obtained from the annealing of a quenched cubic high temperature of sample, is cubic crystal system and lattice $a=14.1243\text{ \AA}$; $Z=4$. The structure refinement converged to $R_p=0.018$, $R_{wp}=0.0212$ $GOF=0.0102$. The structure is built from cationic slabs parallel to (100) faces of the cubic cell. Each cell corresponds to one slab containing a mixed $\text{Bi}_{1.25}\text{V}_{0.123}\text{Ca}_{0.245}$ cationic layer (Bi(1)) sandwiched between two equivalent bismuth layers (Bi(2)). The cohesion of the cations in the slabs results from the presence of the oxygen atoms and nitrogen atoms distributed over three sites. Six O(1) and two O(2) atoms form a slightly distorted cubical polyhedron around the mixed cationic site (Bi(1)). (Bi(2)) atoms are surrounded by seven oxygen nitrogen atoms in a very distorted polyhedron. The important delocalization of (Bi(2)) lone pairs toward the interstitial spaces leads to significant bonds with the adjacent slabs and to the cohesion of the structure. $\text{Bi}_{1.25}\text{V}_{0.123}\text{Ca}_{0.245}\text{O}_8$ is the low symmetry variety of a particular sample of a wide solid solution domain that, formulated $\text{Bi}_{1.25}\text{V}_{0.123}\text{Ca}_{0.245}\text{O}_8$, has been investigated. The formation of this phase from the irreversible transformation of quenched on heating and the subsequent transitions and non-transition metal oxides mixed valence have been evidenced by thermo diffractometry, conductivity measurements versus temperature, dilatometer, and thermal analyses. The morphological study was carried out by SEM.

Keywords: Cubic; *ab initio*; Crystal structure determination; Bismuth vanadium -based mixed oxides; Electronic lone pair; Oxide conductors; Rietveld structure refinement; X-ray diffraction

1. Introduction

A recent investigation of structural and conductivity properties of $\text{Bi}_{1.25}\text{V}_{0.123}\text{Ca}_{0.245}\text{N}_{1.24}\text{O}_8$ oxide conductors which belong to the dimorphic cubic structural-type family has proved close conductivity composition dependence [1]. This has been interpreted on the basis of structural data obtained from Rietveld structure refinements based using JANA software package. The structure is built from cationic slabs parallel to (001) faces of the cubical cells. There are nine formula units $\text{Bi}_{0.775}$, $n_{0.225}$ per octahedral, distributed over three slabs. Each slab is constituted from a mixed $\text{Bi}_{3/n3}$ layer, sandwiched between two Bi_3 layers, and two oxygen sites are located inside; complementary oxide ions, implied by the formulation stoichiometry, are distributed over one or two sites of the inter slab space and exhibit a high mobility, mainly responsible for the conductivity. Depending on the rare-earth nature, a b1 high-temperature form is observed, with a closely octahedral related structure; its formation from the b2 low-temperature variety occurs during a phase transition that has been attributed to a cationic disordering in the mixed $\text{Bi}_{3/n3}$ layers. It is accompanied by sudden increases of both lattice parameters, of oxide occupancy in inter slab spaces, and of the conductivity. The pure ion oxide conductor character of the b1 variety has been clearly demonstrated for the alkaline-earth-based solid solutions and has been also verified for vanadium-based solid. The thickness of the cationic slabs, which is the largest

*Corresponding author: Parashuram Mishra
Bioinorganic and Materials Chemistry Research Lab.M.M.A.M. Campus,Tribhuvan University Biratnagar,Nepal.

for the vanadium term $\text{Bi}_{1.25}\text{V}_{0.123}\text{Ca}_{0.245}\text{N}_{1.24}\text{O}_8$ (the best oxide conductor ever evidenced in this family: at 400 °C is 10^{-3}Scm^{-1} with E 0.8 eV), appears to be an important factor for these attractive conductivity properties. $\text{Bi}_{1.25}\text{V}_{0.123}\text{Ca}_{0.245}\text{N}_{1.24}\text{O}_8$ is a term of a wide solid solution domain, the crystal structure of $\text{Bi}_{1.25}\text{V}_{0.123}\text{Ca}_{0.245}\text{O}_8$ has been determined from powder diffraction data using a combination of direct methods and the novel approach of applying simulated annealing methods simultaneously to X-ray powder pattern by ab initio method. $\text{Bi}_{1.25}\text{V}_{0.123}\text{Ca}_{0.245}$ is a polar, non-centrosymmetric, second harmonic generation active material and its crystal structure is one of the more complex to be solved ab initio from powder diffraction data. Many of the important heterogeneous catalysts are transition and non-transition metals dispersed on oxide supports. Although the primary function of the support is to increase the surface area of the metal, there is now a vast literature documenting that supports can cause pronounced changes in the catalytic and chemisorptions properties of the metal [2]. In particular case, when group 8-10 metals are dispersed on reducible support such as oxide of metal ions. The chemisorptions properties and activity of the catalyst depend on the reduction temperature used for pretreatment. Numerous mechanisms have been proposed to account for this suppression of chemisorptions and the associated change in catalytic activity; the most popular is the diffusion of reduced $\text{Bi}_{1.25}\text{V}_{0.123}\text{Ca}_{0.245}\text{N}_{1.24}\text{O}_8$ moieties onto the metal, thereby blocking metal sites. However, numerous experimental observations are left unexplained by this model. For example, changes in the magnetic properties of V/Ca, composites with reduction temperature indicate that the Bi does not remain as elemental bismuth, but forms a Bi-V-Ca phase [3]. Unfortunately, investigations into the role of compound formation in producing the observed effect have been hindered by the fact that relatively few ternary oxides containing both an early and a late transition and non-transition metal contained mixed valence are known. It is interesting to note that super conductivity has been observed in some of the ternary oxide phases having the Bi and V structure type and for Bi-V-Ca-N-O. In this paper, we report the synthesis and crystal structure of $\text{Bi}_{1.25}\text{V}_{0.123}\text{Ca}_{0.245}\text{N}_{1.24}\text{O}_8$ by ab initio method via powder XRD and also study the morphology and electrical property.

2. Experimental

All chemicals used were analytical grade purchase from Sigma Aldrich U.S.A. A polycrystalline sample of $\text{Bi}_{1.25}\text{V}_{0.123}\text{Ca}_{0.245}\text{N}_{1.24}\text{O}_8$ was synthesized by a standard solid state reaction using a mixture of high purity reagents of $\text{Bi}_2\text{O}_3\text{-NH}_4\text{VO}_3$ and CaCO_3 as the starting materials in the molar ratio of 1:1:1. The mixture was ground carefully, homogenized thoroughly with methanol (99%) in an agate mortar and then packed into an alumina crucible and calcined at 1000 °C in air for 10 h with several intermediate grindings [4]. Finally the product was pressed into pellets and sintered at 100 K/h. Powder X-ray diffraction (XRD) data were collected at room temperature in the angular range of $2\theta = 10$ to 90 with scan step width of 0.02° and a fixed containing time of 15 s using Philips powder diffractometer with graphite monochromatic $\text{CuK}\alpha$ radiation. The powder was rotated during the data collection to minimize preferred orientation effect if any. The program TREOR in CRYSFIRE was used to index the powder pattern which give orthorhombic cell system. SIRPOW92 was used to locate the positional parameters of constituent atoms. The full pattern is fitting and peak decomposition in the space group Pn-3n (222 using check cell program). The structural parameters were refined by the Rietveld method using the JANA program which gave $\text{Rwp}=0.0217$, $\text{Rp}=0.088$, $\text{GOF}=0.012$. The density is determined by Archimedes principle. The morphology of titled compound was determined using SEM. For the electrical studies, the measurements were preceded by a pretreatment of the sample in order to reduce the mean particle size of the obtained powder. After these treatments, the sample achieved about 85% of the theoretical density with the final diameter of 6 mm and thickness of 23mm. The relative density of the sample before the mechanical grinding was 79 %. Platinum electrodes were connected to the two faces of the pellet via a platinum paste to keep good electric contacts. Impedance spectroscopy measurements were carried out using a Hewlett-Packard 4192a Impedance Analyzer. The impedance spectra were recorded in the 5 Hz-13 MHz frequency range. Electrical conductivity measurements of representative $\text{Bi}_{1.25}\text{V}_{0.123}\text{Ca}_{0.245}\text{N}_{1.24}\text{O}_8$ were carried out by complex impedance spectroscopy with an 1174 Solartron frequency response analyzer coupled to a 1266 Solartron electrochemical interface. Pellets of about 14 mm diameter and 1 mm thickness were prepared by cold pressing of a mechanically activated powder mixture with the composition: $\text{Bi}_{1.25}\text{V}_{0.123}\text{Ca}_{0.245}\text{N}_{1.24}\text{O}_8$. To form the phase, the pellets were heated at 700°C during 12 h and slowly cooled to room temperature. This synthesis method was employed to improve the ceramic quality, as it has been shown for other materials [2-6]. The formed phases and crystallinity were studied by X-ray powder diffraction. Platinum electrodes were deposited on the two faces by sputtering, and measurements were carried out in the temperature range 200-650 °C, at steady temperatures, with pellets under air flow and the frequency range was fixed [5].

3. Physical Measurements

X-ray powder diffraction data were obtained on a Philips powder diffractometer using Bragg -Brentano geometry, with a back-monochromatized $\text{CuK}\alpha$ radiation having 1.5456 (Å) wavelengths. Diffraction spectra were scanned by steps of 0.023 (2 θ) over the angle range 5-50 (2 θ), with a counting time of 1.5 s per step. Each sample was rotated 3.14 radian

s⁻¹ during the data recording, in order to minimize the orientation effects resulting from the material compaction [6]. The pattern peak positions are extracted with the Top as P of Bruker-Diffrac 1-64 software package, where each peak profile is refined using the pseudo-Voigt function. The accurate cell parameters of the different samples were refined from 5 to 50 reflections cubic. The crystal structure determination of the phase was carried out for the Philips powder diffractometer Bi_{1.25} V_{0.123} Ca_{0.245} N_{1.24} O₈ parent composition. The first attempts were undertaken by recording X-ray diffraction data, but each time, the intensities diffraction pattern was erroneous by the preferential orientation phenomenon. To minimize the preferential orientation effect and indeed be able to separate the oxygen and N atoms of the heavy atoms Bi and V at room temperature. The crystal structure determination has been concluded by using alternately the JANA (16) and EXPO programs [7]. Dilatometric and conductivity investigations were made on samples pelletized at room temperature (diameter 5 mm, thickness approx. 3 mm), then sintered at 900 °C for 15 h and quenched to room temperature, in liquid nitrogen. The degree of compactness in all cases ranged between 75 and 92%. Dilatometric studies were performed on a Linseis L75 dilatometer with a heating rate of 0.43 C/min between 20 and 700 °C. For conductivity measurements, gold electrodes were vacuum deposited on both at surfaces of the pellets using the sputtering method. The measurements were obtained by impedance spectrometry in the frequency range 1-106 Hz, using a frequency response analyzer Schlumberger 1170; for a given temperature, each set of values was recorded after a 1h stabilization time. The density was calculated by Archimedes principle.

4. Results and discussion

The extensive search for novel inorganic materials with open frameworks formed of tetrahedral and octahedral delimiting inter-layer spaces (2D), tunnels (3D) or cages (1D) where cations are housed, represent currently a field of intense activity including several disciplines: solid-state chemistry, physics, mechanics, and mainly ionic conductivity properties and their use as battery materials oxides of metals and alkaline cations are well known for their thermal stability and the simplicity of syntheses, which is important for many practical applications lithium batteries [7].

The compound was prepared from Bi₂O₃-NH₄VO₃ and CaCO₃ as starting material oxides. Calcium oxide powder was dried and decarbonated at 1000 °C overnight prior to use. The oxides were weighed in stoichiometric proportions and ground together in an agate mortar. The prepared composition was heated up to 1400 °C for overnight in an alumina crucible, no particular condition was used in order to cool down the samples [8]. This procedure was applied at least twice in order to stabilize compound as verified by X-ray powder diffraction. The final compound is white.

4.1. Crystal structure of Bi_{1.25} V_{0.123} Ca_{0.245} N_{1.24} O₈

The framework structure of Bi_{1.25} V_{0.123} Ca_{0.245} N_{1.24} O₈ was first examined by ab initio structure determination method using the powder XRD data shown in figure 1. The initial lattice parameters were determined to be parameters a=14.1243 Å and V=279.7571 Å³ by an indexing procedure using the program TREOR15 in EXPO2004.16. The most probable space group was suggested to be cubic crystal system. Next, the integrated intensities were extracted by the Le Bail method using the program Jana2006 [9]. A profile function and background function of the Le Bail method used in the present study were pseudo-Voigt function and 20th order Legendre function, respectively. An initial structure model was then obtained by the charge flipping (CF) method [17] using the extracted integrated intensities. Although the V site could not be clearly determined by the CF method using the powder XRD data, the framework structure of Bi_{1.25} V_{0.123} Ca_{0.245} N_{1.24} O₈ was successfully determined with the help of Rietveld refinement using JANA package shown in figure 2. Rietveld refinement of cubic crystal system having Pn-3n (222) space group was found with three dimension structure as follows against XRD data shown in figure 3 for structural determination proved difficult, due to a combination of preferred orientation of the plate-like crystallites in flat-plate geometry [10]. In other words, the extracted peak intensities for phase 1 could be reliable. Note that if the relative intensities differed a lot from the simulated patterns of the known phases, additional manual partitioning of those overlapping peaks would be necessary to get reliable intensities for the unknown phase 1. After considering the multiplicity and Lorentz-polarization correction, the intensities of phase 1 were used for the structure solution as below. Moreover, the reflection conditions indicated possible space group.

Pn-3n (222). The initial structure model was obtained using a charge flipping algorithm with the program Superflip 8 [11]. Random phases were used at the beginning of the charge-flipping interaction, and overlapping peaks were re-partitioned using a histogram match to improve the convergence. The iteration converged with an R factor of 29% and the final electron density shows P1 symmetry with a 5% error. The program of EDMA was then used to automatically assign atomic positions. Four unique heavy atomic positions were found and the heaviest one was assigned as Bi while the others were considered as V and Bi. Due to the existence of heavy atoms, all oxygen positions were ambiguous in the electron density map of this stage [12]. To locate the oxygen atoms, a Monte-Carlo based simulated annealing process with the program TOPAS was applied. For each annealing process, various atomic coordinates were randomly

assigned table 2 shown as the initial positions of the oxygen atoms [13]. The annealing process was restarted after finding a few oxygen positions, until all oxygen positions were found to be reasonable with Ca ions. On the whole the crystal structure of cited crystal is octahedral closed face center cubic.

4.2. Crystal symmetry

From the analysis of the X-ray powder diffraction data collected on the MPD-PRO at 1000 °C, we were able to obtain better solutions from two different auto indexing programs Treor [10] and Dicvol implemented in X'Pert High Score Plus. The solutions determined by the both programs are very similar: $a=14.1243 \text{ \AA}$ cubic crystal systems, with a figure of merit (FOM) $M50=30$ and [13] and $M50=65$, respectively, for Treor and Dicvol. From the average oxygen volume in oxides, $V_{\text{oxygen}} = 18-22 \text{ \AA}^3$ at room temperature, and the nominal composition $\text{Bi}_{1.25} \text{V}_{0.123} \text{Ca}_{0.245} \text{N}_{1.24} \text{O}_8$ we can estimate $Z_{\text{max}}=598/18/15=2.39$ and $Z_{\text{min}}=11$. We chose $Z=2$ leading to an oxygen volume slightly larger than the previous values, $V_{\text{oxygen}}=23.3 \text{ \AA}^3$. In order to determine the possible space groups of this compound, an initial procedure was performed to obtain the Bravais class. The observed intensities were extracted using a Le Bail space group $\text{Pn-}3\text{n}$ (222). A Patterson function was then calculated with Gfou implement in the Full prof suite. A strong peak was observed at 0.5, 0.5, and 0 leading to a cubic Bravais class. In the whole the structure of crystal coordinated by octahedral geometry.

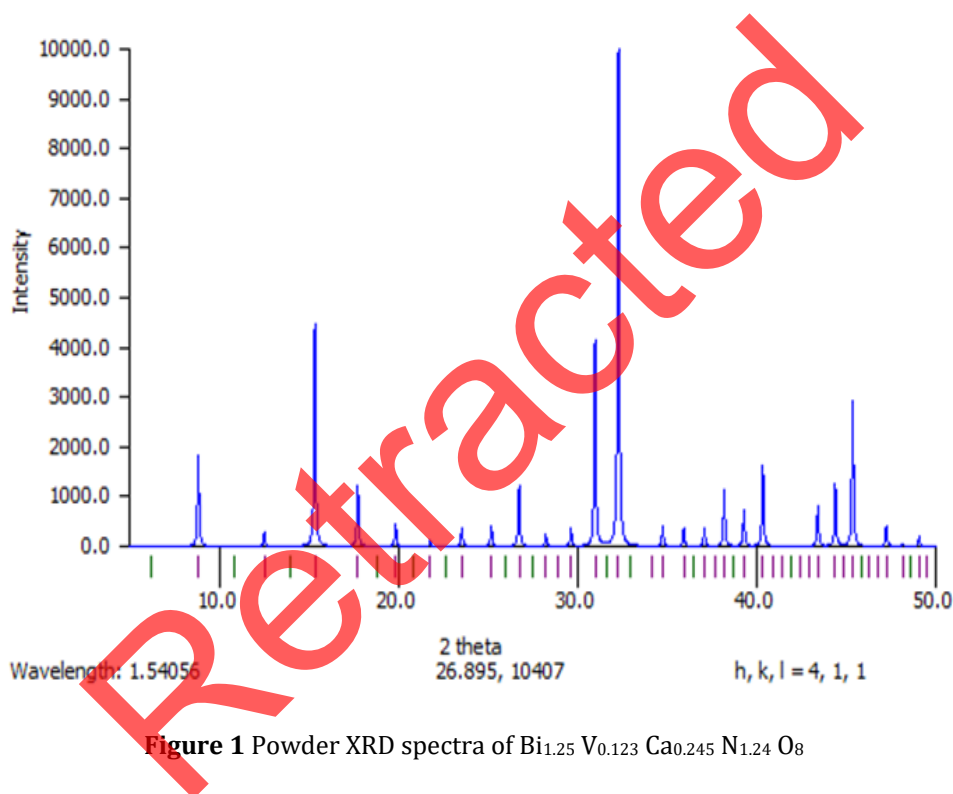


Figure 1 Powder XRD spectra of $\text{Bi}_{1.25} \text{V}_{0.123} \text{Ca}_{0.245} \text{N}_{1.24} \text{O}_8$

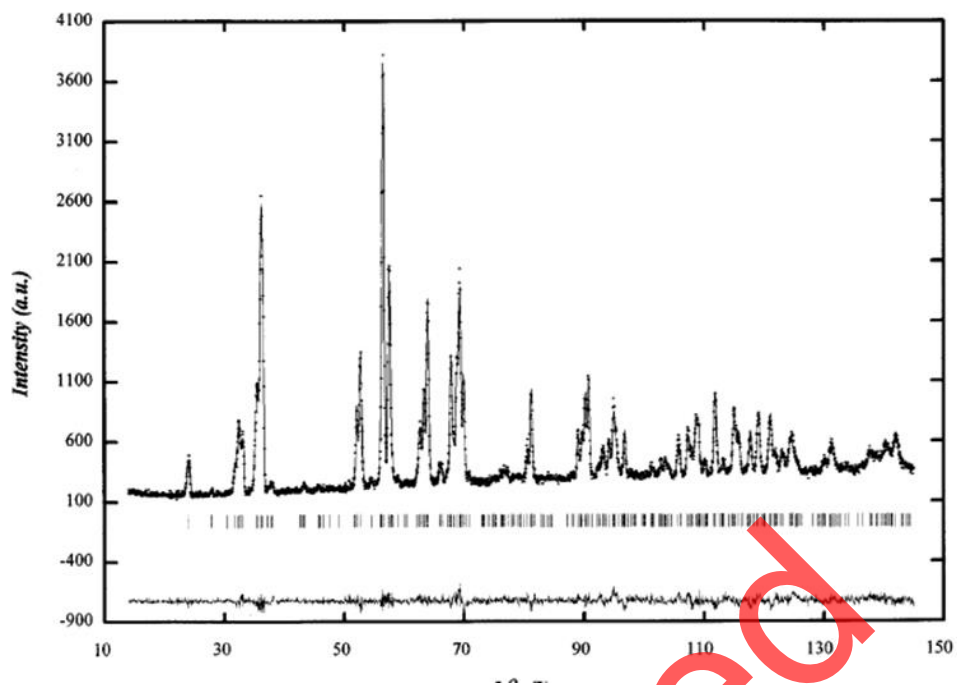


Figure 2 Graphical representation of the result from Rietveld refinement with X-ray powder data. Vertical bars indicate positions of the Bragg reflections for $\text{Bi}_{1.25}\text{V}_{0.123}\text{Ca}_{0.245}\text{N}_{1.24}\text{O}_8$ dots mark the observed intensities and the solid line gives the calculated intensity curve. The deviations between the observed and the calculated intensities from the refined model are shown by the difference plot in the lower part of the diagram.

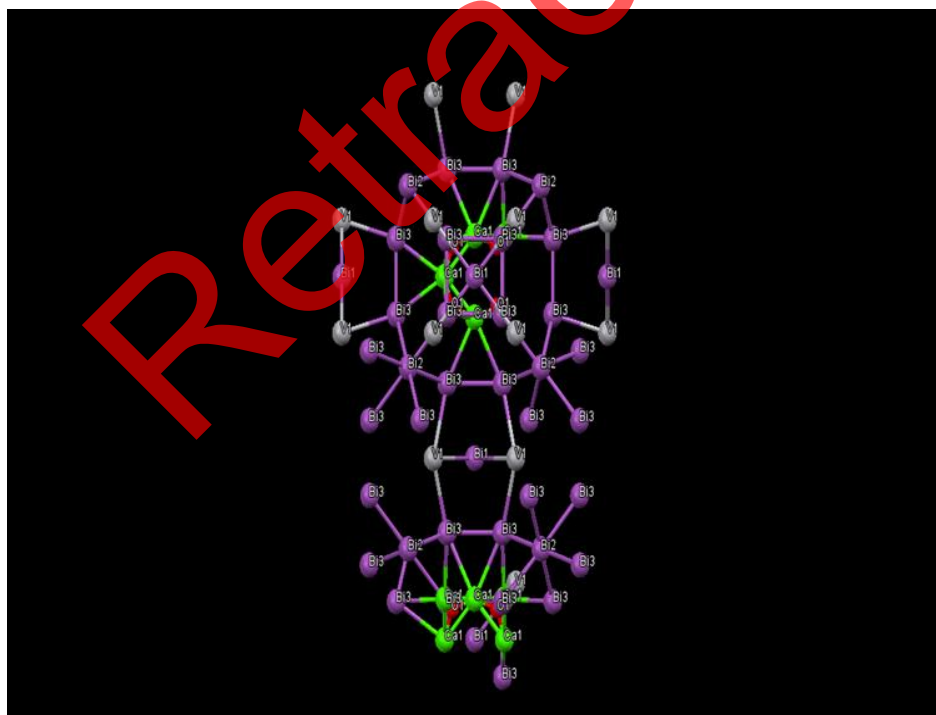


Figure 3 3D structure of $\text{Bi}_{1.25}\text{V}_{0.123}\text{Ca}_{0.245}\text{N}_{1.24}\text{O}_8$

Table 1 Crystallographic data

Formula sum	Bi _{1.25} Ca _{0.145} N _{1.25} O _{4.25} V _{0.123}
Formula weight	358.8 g/mol
Crystal system	cubic
Space-group	P n -3 n (222)
Cell parameters	a=14.1243 Å
Cell ratio	a/b=1.0000 b/c=1.0000 c/a=1.0000
Cell volume	287.74 Å ³
Z	4
Calc. density	10.1488 g/cm ³
Meas. Density	10.1789g/cm ³
Indexes	-1≤h≤3,0≤k≤4,0≤l≤3
Pearson code	cP106
Formula type	N4O19P30
Wyckoff sequence	ihedca
Refine values	Rp =0.0188, Rwp=0.0112, GOF=0.0102

Table 2 Fraction Atomic parameters

Atom	Ox.	Wyck.	Site	x/a	y/b	z/c
Bi2	+3	8c	-.3	1/4	1/4	1/4
Bi3	+3	48i	1	0.29469	0.10513	0.10324
Ca1	+2	24h	..2	0.11215	0.11215	0
O1	-2	16f	.3	0.08490	0.08490	0.08490
V1	+5	24h	..2	1/2	0.15511	0.15511
Bi1	+3	6b	42.2	1/2	0	0
Bi2	+3	8c	-.3.	3/4	-1/4	1/4
Bi3	+3	48i	1	0.70531	-0.10513	0.10324
V1	+5	24h	..2	1/2	-0.15511	0.15511
Bi2	+3	8c	-.3	3/4	1/4	-1/4
Bi3	+3	48i	1	0.70531	0.10513	-0.10324
Ca1	+2	24h	..2	0.88785	0.11215	0
V1	+5	24h	..2	1/2	0.15511	-0.15511
Bi2	+3	8c	-.3.	1/4	-1/4	-1/4
Bi3	+3	48i	1	0.29469	-0.10513	-0.10324
Ca1	+2	24h	..2	0.11215	-0.11215	0
O1	-2	16f	.3	0.08490	-0.08490	-0.08490
V1	+5	24h	..2	1/2	-0.15511	-0.15511
Bi3	+3	48i	1	0.10324	0.29469	0.10513
Ca1	+2	24h	..2	0	0.11215	0.11215
V1	+5	24h	..2	0.15511	1/2	0.15511
O1	-2	16f	.3	-0.08490	-0.08490	0.08490
V1	+5	24h	..2	-0.15511	-1/2	0.15511
Bi3	+3	48i	1	-0.10324	0.29469	-0.10513
Ca1	+2	24h	..2	0	0.11215	-0.11215
O1	-2	16f	.3.	-0.08490	0.08490	-0.08490
Bi3	+3	48i	1	0.10513	0.10324	0.29469
Ca1	+2	24h	..2	0.11215	0.000	0.11215
V1	+5	24h	..2	0.15511	0.15511	1/2
Bi3	+3	48i	1	-0.10513	0.10324	-0.29469
Ca1	+2	24h	..2	-0.112 0.5	0000	-0.11215
Ca1	+2	24h	..2	0.11215	0.000	0.11215
V1	+5	24h	..2	0.15511	0.15511	1/2

The heavy-atom positions M have been refined, whereas the positions of the oxygen atoms have been transformed from the structural model suggested by Lundberg and Sundberg [14]. Each M site was assumed in the refinement as occupied by 0.49 Bi and 0.51V. The calcium sites refined to an occupancy of 0.648(10) for Ca-1 in the 6-sided tunnels and 0.392(8) for Ca-2 inside the 7-sided tunnels. Lattice parameters for a and b axes, determined from a calibrated X-ray diffraction pattern recorded along the [0 0 1] direction, are $a = 14.1243$, $b = 14.1243$, $c = 14.1243$. Reflection intensities I_{hkl} was estimated using the crysfire program. Merging the intensities according to sym-symmetry yielded a data set of 456 crystallographically non-equivalent $hk0$ reflections after removal of 47 symmetry-forbidden reflections with non-zero intensity. The internal R-factor of symmetry-related reflections in the merged data set was 12.8 % with a resolution. According to our analysis space group $Pn3n$ was tried for solving the structure by direct method with the program SIR97 [24]. The program was modified for this purpose with electron scattering factors provided by Jiang and Li [25]. Similar to previous studies [15] suspected dynamical diffraction was taken into account by using a phenomenological compensation based on

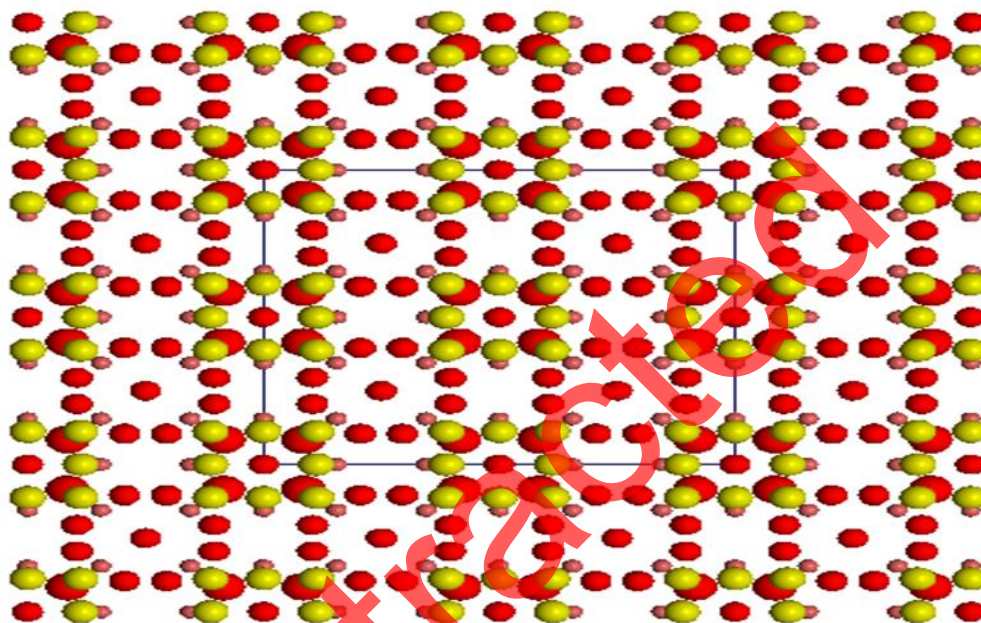


Figure 4 Structure model of $\text{Bi}_{1.25}\text{V}_{0.123}\text{Ca}_{0.245}\text{N}_{1.24}\text{O}_8$ in projection along the short c -axis as obtained from Rietveld refinement with the X-ray powder data.

The heavy Bi and V atoms, which are shown in the figure by the large grey shaded spheres, form with the oxygen atoms (small red spheres) the structural fragments of MO_6 octahedral respectively. The calcium atoms are located inside the 7-(Ca-1) and 6-sided tunnels (Ca-2). The positions of the oxygen atoms have been taken from the proposed structural model of Lundberg and Sundberg and transformed to cubical space group $Pn-3n$. The approximation $|I_{hkl}|/|V_{hkl}|$ that has been derived as the limit for thick crystals under two beam conditions, where V_{hkl} (in volts) designates the structure factor amplitude for electrons. All attempts to use $|I_{hkl}|/|V_{hkl}|^2$ instead led to wrong results with direct methods and least-squares refinement. Moreover, we found that performed geometrical corrections for parallel illumination, as suggested by other authors [16], spoiled the data with the result that it was neither possible to solve the structure nor to refine a given model to good geometry. Following our results obtained for the $\text{Bi}_{1.25}\text{V}_{0.123}\text{Ca}_{0.245}\text{N}_{1.24}\text{O}_8$ nanocrystalline powder, the data were used throughout this study without correction. The most probable solution found with these data by SIR97 had an R-factor of 40%. All 40 heavy atoms in the unit cell are clearly visible in the potential map that was calculated by the program using the 95 largest $hk0$ E-values [16]. Coincidence of several additional weak peaks in the map with suspected oxygen or caesium atoms proved accidental and was not considered as reliable. A (kinematical) least-squares structure refinement on $|V_{hkl}|$ was performed for the detected 11 heavy-atom positions in the asymmetric unit (program SHELXL97-2). For the refinement, it was finally assumed that the heavy-atom positions are fully occupied by tungsten because only this yielded positive defined temperature factors for all atoms. This was not the case if mixed Nb/W sites were assumed and it is an indicator for the presence of dynamical effects. The overall R-factor of the refined framework structure was 39.2% (30 parameters refined, unit weights). The refined atomic coordinates together with the displacement factors U_{eq} are listed in Table 3. The average positional shift of the atoms during the refinement was 0.07\AA (maximum shift 0.11\AA for atom M5). The potential map after least-squares refinement from X-ray diffraction is shown in figure1. An attempt to detect the oxygen positions from a V_{obs}/V_{calc}

difference. Fourier map was unsuccessful due to the relatively high background level (lowest peak to background ratio about 3). Although several diffuse peaks appeared at the expected positions for calcium inside the 6-sided and 7-sided tunnels, the quality of the data did not allow reliable location of these atoms. Thus, the full range of available intensities up to resolution of 0.73 Å was tested. Refinement of the heavy-metal framework with 651 unique reflections and mixed occupancies (Bi/V=1.0) yielded an R-factor of 41.6 %. However, despite several additional peaks appeared in the Vobs-Vcalc differential Fourier map, it was again not possible without knowing the correct positions in advance to assign these peaks to the missing atoms. Since the quality of the received frame work model could not significantly be improved by the data with higher resolution, we present here only the result obtained with intensities up to 1 Å. Nevertheless, in order to check the effect of geometrical correction on the quality of the data, we calculated the required correction factors f_c which match theoretical structure factors V_{hkl} , calc with uncorrected structure factors V_{hkl} , exp, raw and geometrical corrected structure factors V_{hkl} , exp precess corrected, respectively: $f_c = V_{hkl}; \text{calc} = V_{hkl}; \text{exp}; \text{raw}$.

4.3. Crystal structure description

The crystal structure of this compound can be described by different cationic environments. Each mixed site V/Bi(1) is surrounded by eight oxygen atoms (six O(1) atoms and two O(2) atoms) at normal distances ranging from 2.47 to 2.57 Å with a mean distance O/Ca 2.51 Å to form a slightly distorted cubical polyhedron (Fig. 4). This high symmetry of the oxygen environment leads to a very weak stereochemical activity and the nonhybridization of the Bi(1) lone pair (Lp) of the atom, which is likely very close to the bismuth nucleus. The second atom Bi(2) is bonded by seven oxygen atoms to form a very distorted polyhedron, with two very short distances (2.05 and 2.09 Å for respectively the O(3) and O(1) atoms) and normal distances varying from 2.31 to 2.49 Å. This distorted environment is often observed when a Bi atom possesses a lone pair and the refinement of the Bi(2) electronic lone pair Lp2 places it 1.22 Å from the nucleus, to occupy the interlayer between adjacent Bi(2) Ca layers. Each V-Bi(1) atom shares O(1) atoms with the six neighbouring cations V-Bi(1) to form a mixed Ca-Bi-O layer parallel to the plan (b, c), associated with angles shown in table 4. In the same manner, each Bi(2) atom shares also oxygen atoms with the six closest bismuth atoms, to form a layer parallel to the precedent (Fig. 4b). Thus, the crystal structure can be described by a piling of layers ABC, ABC, etc., in the a-axis direction, where layers A and C are formed by Bi(2) atoms and their oxygen environment, and layer B is constituted by mixed sites La}Bi(1) and their oxygen atoms (Fig. 5). The cohesion between layers A and B is ensured by the O(1) and O(2) atoms with long distances to the Ca-Bi -V(1) atoms (Fig. 4) and all bond angles are shown in table 3.

Table 3 Selected Bond angles

Number	Atom 1	Atom 2	Atom 3	Atom 4
1	Bi2	Bi3	Bi3	132.86
2	Ca1	Bi3	V1	158.51
3	Ca1	Bi3	Ca1	44.30
4	V1	Bi3	Ca1	157.14
5	V1	Bi3	Bi3	103.91
6	V1	Bi3	Bi3	103.15
7	Ca1	Bi3	Bi3	92.16
8	Ca1	Bi3	Bi3	60.07
9	O1	Ca1	Bi3	77.69
10	O1	Ca1	Ca1	31.73
11	O1	Ca1	Ca1	115.92
12	O1	Ca1	Ca1	31.73
13	O1	Ca1	Ca1	115.92
14	O1	Ca1	Bi3	133.83
15	O1	Ca1	O1	131.16
16	O1	Ca1	Bi3	134.01
17	Bi3	Ca1	Ca1	67.51

18	Ca1	Ca1	Bi3	67.51
19	Bi3	Ca1	O1	78.26
20	Bi3	Ca1	Bi3	79.66
21	O1	Ca1	Bi3	77.69
22	Ca1	O1	Ca1	116.54
23	Ca1	O1	Ca1	116.54
24	Ca1	O1	Ca1	116.54
25	Bi3	V1	Bi3	70.67
26	Bi3	V1	Bi3	141.34
27	Bi1	V1	Bi3	70.67
28	V1	Bi1	V1	90.00
29	V1	Bi1	V1	90.00
30	Ca1	Ca1	Ca1	60.00
31	Ca1	Ca1	Bi3	164.75
32	Ca1	Ca1	O1	115.92
33	Ca1	Ca1	Bi3	108.92
34	Bi3	Ca1	Ca1	105.50
35	Bi3	Ca1	Ca1	108.92
36	Ca1	Ca1	Ca1	120.00
37	Ca1	O1	Ca1	116.54
38	Ca1	O1	Ca1	116.54
39	Ca1	O1	Ca1	116.54
40	Ca1	O1	Ca1	116.54
41	N2	v	Ca1	116.54
42	N1	Bi1	V1	180.00
43	N1	Bi1	V1	180.00

5. Morphological study by SEM (Scanning electron microscopy)

Scanning electron microscopy (SEM) is giving morphological examination with direct visualization. The techniques based on electron microscopy offer several advantages in morphological and sizing analysis; however, they provide limited information about the size distribution. For SEM characterization, nanoparticles solution should be first converted into a dry powder, which is then mounted on a sample holder followed by coating with a conductive metal, such as gold, using a sputter coater [17]. The sample is then scanned with a focused fine beam of electrons. The surface characteristics of the sample are obtained from the secondary electrons emitted [18] from the sample surface. The morphology of the oxide nanoparticles is shown in Figure 5. From the image, it is clear that the particles were highly agglomerated in nature. The SEM pictures clearly show randomly distributed grains with smaller size. From the SEM analyses, one can conclude the formation of nanoparticles spherical structure. Here it is grown in very high-density and possessing almost uniform spherical shapes. The image reveals that the average size of the particles is 20.32 nm.

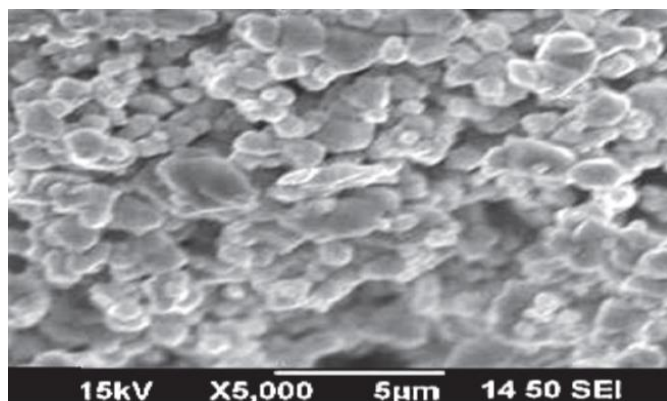


Figure 5 SEM spectrograph of $\text{Bi}_{1.25}\text{V}_{0.123}\text{Ca}_{0.245}\text{N}_{1.24}\text{O}_8$

The sample is then scanned with a focused fine beam of electrons. The surface characteristics of the sample are obtained from the secondary electrons emitted [12] from the sample surface. The morphology of the oxide nanoparticles is shown in Figure 5. From the image, it is clear that the particles were highly agglomerated in nature. The SEM pictures clearly show randomly distributed grains with smaller size. From the SEM analyses, one can conclude the formation of nanoparticles spherical structure. Here it is grown in very high-density and possessing almost uniform spherical shapes. The image reveals that the average size of the particles is 25.32 nm.

5.1. Electrical properties

The electrical properties of the title compounds were determined by using complex impedance spectroscopy. The electrical measurements were carried out in air in the 240–360°C temperature range after stabilization at each step of 30 °C and in the frequency range 1Hz-13MHz. The applied voltage was 0.5 V, which allows eliminating aberrant points at low frequencies. Z-view computer program [19] was used to determine the electrical parameters by using a conventional electrical circuit as follow: $R//CPE-R//CPE$, where CPE is a constant phase element:

$$Z_{CPE} = \frac{1}{A(j\omega)^p} \dots\dots\dots 1$$

An additional inductance L was added to account for instrumental contributions especially at high temperature. The true capacitance was calculated from the pseudo-capacitance according to the following relationships

$$\omega_o = (RA)^{-1/P} = (RC)^{-1} \dots\dots\dots 2$$

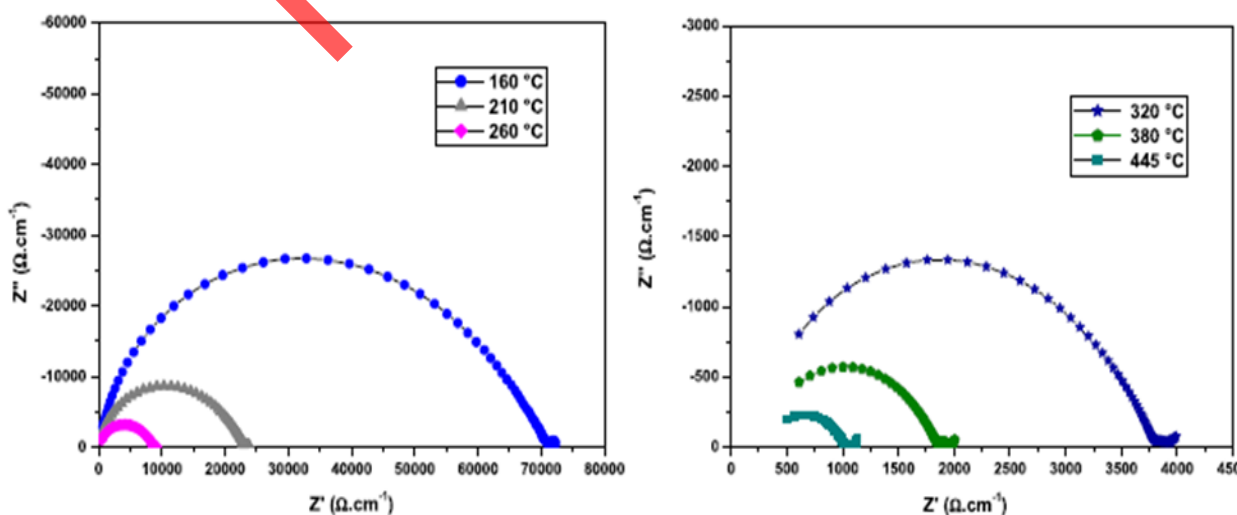


Figure 6 Normalized impedance spectra recorded on $\text{Bi}_{1.25}\text{V}_{0.123}\text{Ca}_{0.245}\text{N}_{1.24}\text{O}_8$ at 160°C – 445°C.

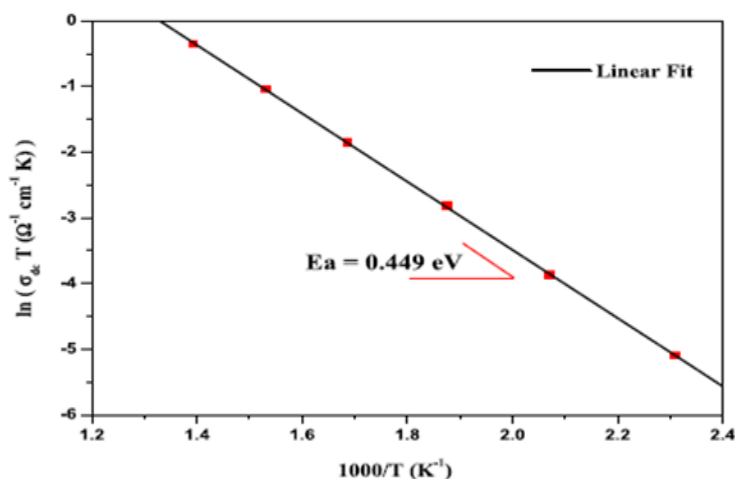


Figure 7 Arrhenius plots of conductivity of $\text{Bi}_{1.25}\text{V}_{0.123}\text{Ca}_{0.245}\text{N}_{1.24}\text{O}_8$.

Table 4 Electrical values of the equivalent circuit parameters calculated for $\text{Bi}_{1.25}\text{V}_{0.123}\text{Ca}_{0.245}\text{N}_{1.24}\text{O}_8$ sample at different temperatures.

T (°C)	T (K)	$C_1(\times 10^{-11} \text{ F}) \pm 0.02$	$P1 \pm 0.02$	$P(k\ \Omega\ \text{cm}) \pm 0.01$	$\sigma(\times 10^{-4} \text{ S}\cdot\text{cm}^{-1}) \pm 0.01$
160	433	1.49	0.9	78.832	0.14
210	483	1.51	0.9	23.263	0.43
260	533	1.64	0.9	8.958	1.11
320	593	1.59	0.9	3.788	2.64
380	653	1.58	0.8	1.852	5.40
445	718	1.70	0.8	1.022	9.78

Geometric value of pellet $g=0.812 \text{ cm}^{-1}$

normalized impedance spectra recorded on $\text{Bi}_{1.25}\text{V}_{0.123}\text{Ca}_{0.245}\text{N}_{1.24}\text{O}_8$ at $160^\circ\text{C} - 445^\circ\text{C}$ are shown in figure 6. The electrical parameters values achieved from the equivalent circuit in the temperature range $160^\circ\text{C} - 445^\circ\text{C}$ are summarized in Table 4 where, the resistivity $\rho=R/k$ is extracted from the refinement of each contribution which the geometric factor of the cylindrical pellet $g(\text{cm}^{-1})=e/S$ (e =thickness; S =surface). The conductivity increases from $0.14 \times 10^{-4} \text{ Scm}^{-1}$ at 160°C - $9.78 \times 10^{-4} \text{ Scm}^{-1}$ at 445°C (Table 4). Although, the absolute conductivity value of the Al/Li-substituted title material at 320°C ($\sigma=2.64 \times 10^{-4} \text{ Scm}^{-1}$). The Arrhenius plot of the electrical conductivity, $\log(\sigma T)$ ($\text{S}\cdot\text{Kcm}^{-1}$) as a function of $1000/T$ (K^{-1}), in the temperature interval $160^\circ\text{C} - 445^\circ\text{C}$ is illustrated in Figure 7. As a single linear plot and following the Arrhenius law, the activation energy of the $\text{Bi}_{1.25}\text{V}_{0.123}\text{Ca}_{0.245}\text{N}_{1.24}\text{O}_8$ compound determined by linear fit is 0.549 eV and show pseudo - order of kinetic thermal reaction. Its conductivity increases with increasing temperature. This material presents interesting electrical performance and can be used as super-conductor materials.

6. Conclusion

The title compound, $\text{Bi}_{1.25}\text{V}_{0.123}\text{Ca}_{0.245}\text{N}_{1.24}\text{O}_8$ has been synthesized as polycrystalline powder by solid-state method. To the present authors' knowledge, our work is the first to uncover the metal framework structure of a large unit cell heavy-metal oxide contained mixed valence with tunnel structure directly from single-projection X-ray diffraction data. To reach this goal, large-angle precession X-ray diffraction intensities have been collected on imaging plates at 100 kV . Processing of the data was performed following the quasi-kinematical approach as outlined elsewhere. Suggested data correction schemes for the geometry of off-axis hollow-cone illumination have been checked, but were not applied because this impaired the quality of the data. Thus, the framework structure of the title compound was solved from uncorrected data with 1A° resolution using the direct methods program SIR97. All atoms in the asymmetric unit of the $\text{Bi}_{1.25}\text{V}_{0.123}\text{Ca}_{0.245}\text{N}_{1.24}\text{O}_8$ framework were readily found by the program and correctly assigned with their 3D coordinates. A (kinematical) least-squares structure refinement of the heavy-atom positions was carried out with the program JANA using the same $h\ k\ o$ data set. Comparison of the refined co-ordinates for the heavy atoms resulting from Rietveld refinement on X-ray powder data (present study) showed an average agreement for the metal framework structure within 0.09 \AA . SEM analysis of several crystallites examined indicates an average chemical composition of this phase according to $\text{Bi}_{1.25}\text{V}_{0.123}\text{Ca}_{0.245}\text{N}_{1.24}\text{O}_8$. Despite the quality of the available precession X-ray diffraction data proved sufficient for accurate determination of the heavy-atom positions, the data quality did not allow to

unambiguously locate the vanadium atoms inside the tunnels nor to reveal the oxygen atoms. Theoretical calculations carried out for the M5O14 framework structure show that simple formulas for the detectability of light atoms in the presence of heavy atoms can be misleading, since the background noise which results from truncation errors in the Fourier synthesis is not taken into account. Thus, for calculated data with 1 \AA resolution it was found that the heavy atoms appear effectively 7.8 times stronger in the projected map than the oxygen. This explains why it would be very difficult with real data to detect the oxygen and nitrogen positions, in particular if only data from a single zone axis are considered as in the present case. The fact that it was neither possible to detect the oxygen nor the calcium atoms in the structure is a strong indicator that the data from precession X-ray diffraction still contain considerable amounts of dynamical/secondary scattering. This is also displayed by the relatively large R-factors after LS-refinement (39.2%). From our point of view, the fact that it was possible to determine the heavy-atom positions with high precision even from 100 kV data is yet a great success, because solving these types of heavy-metal framework structures directly from X-ray diffraction data was attempted by several groups for many years, but obviously, without success. Therefore, the present result is a striking example where precession X-ray diffraction reduced dynamical diffraction below the critical limit at which the determination of the structure or, at least, a fundamental part of it is enabled. However, further experiments which address to optimized conditions for detecting the oxygen atoms in heavy-atom structures seem to be necessary. So collection of 3D intensity data are likely more promising to reach this goal, since such extended data sets proved sufficient to detect even the most light atom, oxygen and nitrogen atoms. So from the above discussion we concluded that the structure of cited compound by powder pattern and the particle show nanomaterial can be used in super conductor.

Compliance with ethical standards

Acknowledgments

The authors would like to acknowledge the immense contribution Department of Chemistry, University of Delhi, India for laboratory facility.

Disclosure of conflict of interest

The authors declare that they have no conflict of interest.

References

- [1] Thomas E Weiricha, Joaquim Portillob C, Gerhard Coxd, Hartmut Hibste, Stavros Nicolopoulosb. Ab initio determination of the framework structure of the heavy-metal oxide $\text{CsxNb}_{2.54}\text{W}_{2.46}\text{O}_{14}$ from 100 kV precession electron diffraction data, *Ultramicroscopy*. 2006; 106: 164–175.
- [2] Zhengyang Zhou, Lukáš Palatinus, Junliang Sun. Structure determination of modulated structures by powder X-ray diffraction and electron diffraction *INORGANIC CHEMISTRY FRONTIERS*. 2019.
- [3] T Dan Vu, Firas Krichen, Maud Barre, Sandrine Coste, Alain Jouanneaux, Emmanuelle Suard, Andrew Fitch, François Goutenoire. Ab Initio Structure Determination of $\text{La}_{34}\text{Mo}_{80}\text{O}_{75}$ Using Powder X-ray and Neutron Diffraction Data *Cryst. Growth Des.* 2020.
- [4] Bimal K kanth, Parashuram Mishra. Synthesis and structure determination of novel mixed valence $\text{Pb}_{0.5}\text{U}_{0.25}\text{Zr}_{1.25}\text{O}_{4.5}$ by powder xrd obtained from $\text{PbCO}_3\text{-U}(\text{CO}_3)_2\text{-Zr}(\text{CO}_3)_2$ ternary mixed valence oxides, *International journal for research in applied and natural science*. 2020; 6(7).
- [5] Manickam Minakshi, David RG Mitchell, Christian Baur, B Johann Chable, Anders J Barlow, Maximilian Fichtner, Amitava Banerjee, Sudip Chakraborty, Rajeew Ahuja. Structure Determinations of Two New Ternary Oxides: Ti_2PdO and $\text{Ti}_2\text{Pd}_2\text{O}_7$, *Nanoscale Adv.* 2019; 1: 565.
- [6] J You, L Xin, X Yu, X Zhou, Y. Liu. Synthesis of homogenous CaMoO_4 microspheres with nanopits for high-capacity anode material Li-ion battery, *Appl. Phys.A: Mater. Sci. Process.* 2018; 124: 271-580.
- [7] Y Liang, X Han, Z Yi, W Tang, L Zhou, J Sun, S Yang, Y Zhou. Synthesis, characterization and lithium intercalation properties of rod-like CaMoO_4 nanocrystals, *J. Solid State Electrochem.* 2007; 11: 1127–1131.
- [8] Parashuram Mishra. Synthesis, crystal structure determination and ionic properties of novel $\text{BiCa}_{0.5}\text{Mg}_{0.5}\text{O}_{2.5}$ via X-ray powder diffraction data *Crystal Growth*. 2014; 2041(32): 2041-204.

- [9] Michael James, Melody L. Carter, Zhaoming Zhang, Yingjie Zhang, Kia S. Wallwork, JMaxim Avdeev and Eric R. Vancez. Crystal Chemistry and Structures of (Ca,U) Titanate Pyrochlores J. Am. Ceram. Soc., 93 [10] 3464–3473 (2010)
- [10] N Tancret, S Obbade, N Bettahar, F Abraha. Synthesis of Ternary Metal Oxides for Battery-Supercapacitor Hybrid Devices: Influences of Metal Species on Redox Reaction and Electrical Conductivity. Journal of solid state chemistry. 1996; 124: 309–318.
- [11] T Dan Vu, Firaskrichen, Maud Barre, Sandrine Coste, Alain Jouanneaux, Emmanuelle Suard, Andrew Fitch, FrançoisGoutenoire.
- [12] Chambrier M, Bail A. L, Giovannelli F, Redjaimia A, Florian P, Massiot D, Suard E, Goutenoire, F. La₁₀W₂O₂₁: An Anion-Deficient Fluorite-Related Superstructure with Oxide Ion Conduction. *Inorg. Chem.* 2014; 53,1:147–159.
- [13] Lopez-Vergara A, Porrás-Vázquez JM, Infantes-Molina A, Canales -Vázquez J, Cabeza A, Losilla ER, Marero-Lopez D. Effect of Preparation Conditions on the Polymorphism and Transport Properties of La_{6-x}MoO_{12-δ} (0 ≤ x ≤ 0.8). *Chem. Mater.* 2017; 29: 6966–6975.
- [14] Dubois F, Goutenoire F, Laligant Y, Suard E, Lacorre P. Ab-Initio Determination of La₂Mo₄O₁₅ Crystal Structure from X-rays and Neutron Powder Diffraction. *J. Solid State Chem.* 2001; 159: 228–233.
- [15] Bimal K. Kanth, Parashuram Mishra. Synthesis and Ab Initio Determination Bi_{1.256} La_{0.53} N_{0.231} O_{0.521} Zr_{1.543} Triclinic Structure from Powder X-Ray Diffraction Data, *Sch Int J Chem Mater Sci*, July, 2020; 3(6): 6
- [16] DO Charkin. Modular approach as applied to the description, prediction, and targeted synthesis of bismuth oxohalides with layered structures, *Russ. J. Inorg. Chem. Suppl.* 2008; 53: 1977–1996.
- [17] G Kresse, D Joubert. From ultra-soft pseudopotentials to the projector augmented wave method, *Phys. Rev. B.* 1999; 59: 1758–1775.
- [18] Minfeng Lü, Marie Colmont, Houria Kabbour, Silviu Colis, Olivier Mentré. Revised Bi/M Layered Oxo-Sulfate (M = Co, Cu): A Structural and Magnetic Study. *J. Inorg. Chem.* 2014; 53: 6969–6978.
- [19] Riadh Marzouki, Youssef Ben Smida, Manel Sonni, Maxim Avdeev, Mohamed Faouzi Zid. Synthesis, structure, electrical properties and Na⁺ migration pathways of Na₂CoP_{1.5}As, *Journal of Solid State Chemistry.* 2019.

Author's short biography

Parashuram Mishra

Parashuram Mishra is a senior researcher and did Postdoc from University of Delhi, India. He involved in teaching and research more than 25 years and awarded by Science and Technology Award from Govt. of Nepal as well as Outstanding International Scientist Award also.

Rohit Kumar Dev

Rohit Kumar Dev is a Ph.D. research scholar doing under Prof. Parashuram Mishra, Tribhuvan University, Bio-inorganic and Materials Chemistry Lab. M. M. A. M. Campus, Biratnagar, Nepal.